1-1-2009

Photothermal effect in narrow band gap PbTe semiconductor

Z. Dashevsky

V. Kasiyan

S. Asmontas

J. Gradauskas

E. Shirmulis

See next page for additional authors

Journal of Applied Physics

Photothermal effect in narrow band gap PbTe semiconductor

Cite as: J. Appl. Phys. **106**, 076105 (2009); https://doi.org/10.1063/1.3243081
Submitted: 13 July 2009 . Accepted: 08 September 2009 . Published Online: 13 October 2009

Z. Dashevsky, V. Kasiyan, S. Asmontas, J. Gradauskas, E. Shirmulis, E. Flitsiyan, and L. Chernyak

Photothermal effect in narrow band gap PbTe semiconductor

Z. Dashevsky,[1] V. Kasiyan,[1] S. Asmontas,[2] J. Gradauskas,[2] E. Shirmulis,[2] E. Flitsiyan,[3] and L. Chernyak[3,a)]
[1]*Department of Materials Engineering, Ben-Gurion University of the Negev, Beer-Sheva 84105, Israel*
[2]*Semiconductor Physics Institute, A. Gostauto 11, Vilnius 2600, Lithuania*
[3]*Department of Physics, University of Central Florida, Orlando, Florida 32816-2385, USA*

(Received 13 July 2009; accepted 8 September 2009; published online 13 October 2009)

In this paper we report the observation of photothermal effect in PbTe *p-n* junction. The effect is expressed in photosignal generation due to illumination by 100 ns pulse CO_2 laser with photon energy less than PbTe forbidden gap. © *2009 American Institute of Physics*.
[doi:10.1063/1.3243081]

Lead telluride (PbTe) is a narrow band gap semiconductor with an energy gap $E_g = 190$ meV at $T = 0$ K. PbTe and a wide range of its solid solutions represent a group of materials that are extensively used in different fields of opto- and microelectronics, thermoelectricity, and even as gas sensors.[1] Because the band gap of PbTe corresponds to the infrared (IR) spectral region of 3–5 μm, a PbTe *p-n* junction is often considered as a promising middle IR-detector.[2] Recently we reported the observation of pyroelectric effect (PRE) in PbTe *p-n* junction.[3] This effect is due to a temperature-dependent electric dipole in a nonpolar semiconductor. The junction was illuminated by modulated (4–200 Hz) CO_2 laser beam with ~ 1 W/cm^2 intensity. The pyroelectric signal with the magnitude of ~ 10–20 μV and polarity, which changed in the dark phase, has been observed.

In this paper we report a photosignal (PS) from PbTe *p-n* junctions under CO_2 single-pulse (100 ns duration) laser excitation. The PS shape differs from that previously reported by us in Ref. 3: After laser illumination the PS decreases to zero on microsecond scale without changing its polarity.

Two types of *p-n* junctions have been studied in this work. These junctions differ by the method used to create the *n*-region "pocket" within the *p*-type PbTe ingot. While the first method used In_4Te_3 gas diffusion [thermally diffused junctions (TDJs)], the other employed ion implantation [implanted junctions (IJs)]. Schematics of both types of *p-n* junctions are presented in Fig. 1.

PbTe crystals were grown by a Czochralski technique.[4] A ⟨100⟩-oriented PbTe-seed was used for growth. To prevent decomposition of the melt, liquid encapsulation by about 1–cm-thick molten B_2O_3 layer was employed. The crystals were grown with excess of Te (up to 0.3 at. %), which leads to acceptor point defects (Pb vacancies) with zero activation energy.[4] These defects were quenched-in by sufficiently rapid cooling, to inhibit their contribution to the electrical conductivity. The Hall effect was employed for direct measurements of free carrier concentration. The acceptor concentration, N_a, in as-grown crystals was $\approx 10^{18}$ cm^{-3}. The saturation mobility, μ_{sat}, was 10^6 cm^2/V s at 4.2 K, which indicates a high quality of PbTe crystals.[5]

Rectangular wafers ($20 \times 10 \times 1$ mm^3) used in this research were cut from a single-crystal ingot. One of the sides of these wafers has been successively polished mechanically and electrochemically.[5] Thermally diffused doping was accomplished by exposing the sample to indium from In_4Te_3 gaseous source. The concentration of In-dopant was in the 0.1–0.5 at. % range and was varied by changing the exposure time (1–5 h) and annealing temperature (from 500 to 600 °C). Unique properties of In-doped PbTe are related to the effect of Fermi level pinning.[6] In the latter case, a stable free carrier concentration is achieved, independent of indium concentration variation in the sample. At 4.2 K, the Fermi level is pinned at 70 meV above the conduction band edge, giving rise to the electron density of 6×10^{18} cm^{-3}.

For IJ structures, an oxide layer has been electrochemically formed and subsequently patterned on a polished wafer side [see Fig. 1(b)]. The samples were uniformly implanted by 200 keV Zn ions with a dose of 1×10^{16} ions/cm^2. This allowed intrinsic diffusion of implantation-induced Te vacancies (donors in PbTe) leading to homogeneous electron concentration of $\sim 6 \times 10^{18}$ cm^{-3} across a 4-μm-thick sample.[5]

To determine location of *p-n* junction within the sample, a method for measuring the local Seebeck coefficient along the surface of the doped crystal was used.[5] Seebeck coefficient variations were measured along a direction normal to the external surface and the *p-n* junction depth was obtained

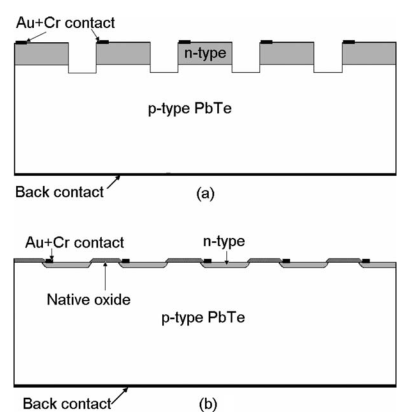

FIG. 1. Schematic view of the *p-n* junction diode array. (a) Mesa columns of TDJ. (b) The planar array of IJs, formed by ion implantation through the windows in the oxide layer.

a)Electronic mail: chernyak@physics.ucf.edu.

TABLE I. Main properties of PbTe diodes.

Type of diode	Temperature (K)	Resistance at zero bias, R_0 (Ω)	Capacitance, C (nF)	R_0C time constant, τ (s)
TDJ	80	1.30×10^5	7.00	9.1×10^{-4}
TDJ	110	1.10×10^4	6.35	6.98×10^{-5}
TDJ	140	540	5.7	3.08×10^{-6}
TDJ	180	59	5.5	3.25×10^{-7}
IJ	80	1.24×10^4	14.4	1.79×10^{-4}
IJ	100	1.00×10^4	14.2	1.42×10^{-4}
IJ	140	103	13.9	1.43×10^{-6}
IJ	180	14.6	⋯	⋯

from a change in Seebeck coefficient polarity. While for IJ crystals a junction was located at the depth of several microns under the PbTe surface, for TDJ crystals the depth of about 70 μm counting from the top surface was obtained.

Capacitance-voltage (C-V) and current-voltage (I-V) curves were measured over 12–200 K temperature range. The investigated samples were placed in a closed-cycle He-gas cryostat under the pressure of $\sim10^{-7}$ Torr. The temperature stability was at the level of 0.02 K above 100 K. I-V characteristics of p-n junctions were obtained by varying bias voltage between −1 and +0.3 V with measurements being taken every 0.2 mV. A QuadTech 1920 *LCR*-meter was used for C-V measurements. The capacitance was measured using an alternating signal of 20 mV at 1 MHz, with reverse bias voltage between 0 and 1 V with measurements taken every 2 mV.

The junction was illuminated by Q-switched CO_2 laser beam with the wavelength of 9.5 μm, pulse duration of 100 ns, and maximum intensity of about 0.1 MW/cm^2. The laser beam was focused by a ZnSe lens down to a diameter of ~1 mm. The observed photoelectric response was measured as a function of temperature, reverse bias voltage, and laser beam intensity. The temporal response from a p-n junction has been measured by Tektronix differential preamplifier ADA400A and displayed using Tektronix e-Scope TDS 3054B. The laser pulse duration was measured using a Ge:Au detector.

I-V and C-V characteristics of TDJ and IJ structures are presented in Ref. 7. In this paper, the values for capacitance and resistance at zero bias (R_0) are summarized in Table I for the 80–180 K temperature range. The *RC* time constant ($\tau=R_0\times C$) is also given in Table I. The linearity of C^{-3} versus bias indicates that both types of junctions are linearly graded.[7] While for TDJ structure the rectifying properties are observed up to 180 K, the IJ structure exhibits p-n characteristics up to 140 K. The experimental I-V curves have been fitted with Schokley formula,

$$I=I_0\left[\exp\left(\frac{eV}{nkT}\right)-1\right], \tag{1}$$

where I_0 is the saturation current, n is the ideality factor; k is the Boltzmann constant, and T is the absolute temperature. At $T\geq80$ K the ideality factor n is close to 2, which demonstrates that the dominant generation-recombination process in p-n junction is similar to that in the Schottky barrier on PbTe epitaxial film.[8] At 80 K, the barrier height eV_0 for both types of diodes is close to the energy gap E_g (for PbTe, $E_g\approx210$ meV at 80 K) and eV_0 decreases sharply with increasing temperature. For TDJ structure, eV_0 is on the level of 80 meV at 180 K. For IJ structure, the barrier flattens at 140 K.

The PS for both types of p-n junctions, compared to that from Ge:Au detector, is displayed in Fig. 2 at 90 K. Note that the polarity of p-n junction PS is consistent with that for photovoltaic effect, which could be induced in p-n junction under proper illumination. Figure 2 also shows the PS predicted in accordance with Eq. (2) (see below) for TDJ structure.

The low temperature (90 K) photoresponse as a function of bias for TDJ structure is shown in Fig. 3(a). The PS disappears at the forward bias close the barrier height eV_0. The PS as a function of the incident radiation power P/P_0 ($P_0=1$ kW) at 90 K is shown in Fig. 3(b) for TDJ structure. The PS grows over the whole power range and approaches saturation at the maximum power. The PS versus temperature for two types of structures is presented in Fig. 4. Note that the PS maximum decreases with increasing temperature due to decreasing barrier height. In TDJ structure, for example, the PS persists for up to 180 K, consistent with observation of rectifying properties for this type of p-n junction.

The model that accounts for the effect of PS generation (also known as photothermal effect) consists of the following steps:

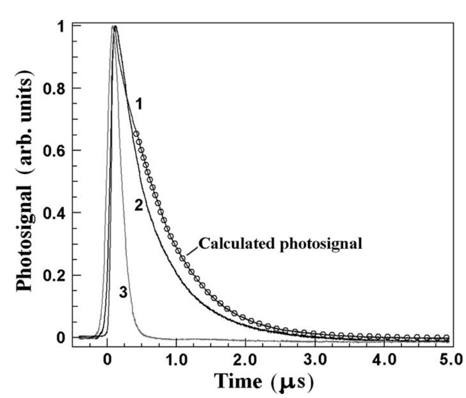

FIG. 2. PS for PbTe p-n junction structures [(1) TDJ, (2) IJ] and reference detector Ge:Au (3) at 90 K. The PS, calculated in accordance with Eq. (2), is shown for TDJ.

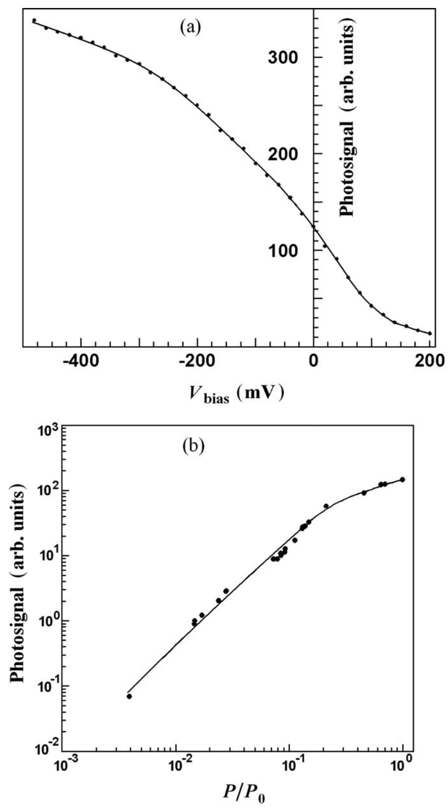

FIG. 3. (a) PS from TDJ structure at $T=90$ K vs bias voltage. (b) PS from TDJ structure at $T=90$ K as a function of CO_2 laser intensity.

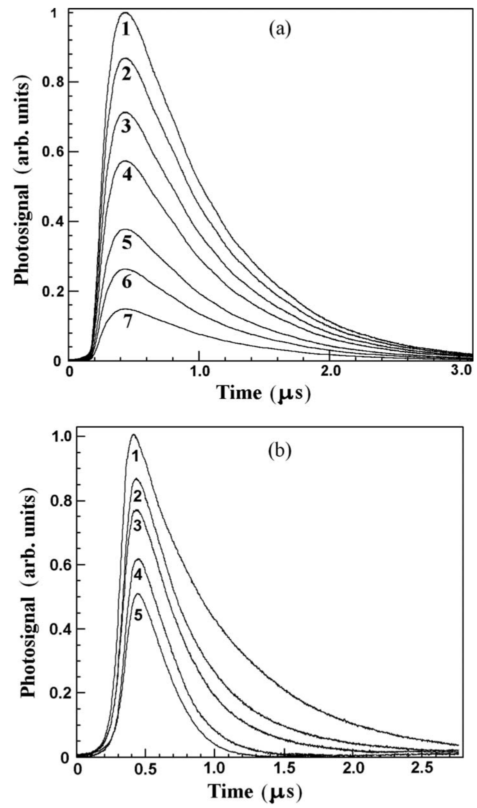

FIG. 4. PS from PbTe *p-n* junction structures as a function of temperature. (a) TDJ: (1) 90, (2) 100, (3) 120, (4) 140, (5) 160, (6) 170, and (7) 180 K. (b) IJ: (1) 90, (2) 100, (3) 110, (4) 120, and (5) 140 K.

- strong laser pulse (IR-photons) absorption on free carriers [in PbTe, the absorption coefficient on free carriers is $\sim 3\times 10^4$ cm^{-1} at $\lambda \approx 10$ μm and $n \sim 5 \times 10^{18}$ cm^{-3} (Ref. 9)] induces heating of the electron system in a 2–3-μm-thick layer;
- heat transfer from the "hot electrons" to the phonon system within a characteristic time of $\sim 10^{-11}$ s (Ref. 10);
- localized temperature rise and consequent thermal generation of nonequilibrium electron-hole pairs that diffuse toward *p-n* junction;
- separation of electron-hole pairs on *p-n* junction built-in electric field (this effect is reminiscent of *p-n* junction photovoltaic effect);
- recombination of electron-hole pairs after laser pulse.

The back PS front, which is associated with recombination of electron-hole pairs, is described as

$$V(t) = V_{\max} \exp\left(-\frac{t}{\tau}\right), \qquad (2)$$

where $V_{\max}$ is the PS amplitude, t is the current time, and τ is the decay constant.

Fitting the experimental results with Eq. (2) gave the decay constant of ~ 0.5 μs for TDJ structure (see Fig. 2).

We observed the photothermal effect in the narrow band gap PbTe *p-n* junctions under far-IR CO_2-laser irradiation. This effect was induced due to generation of nonequilibrium electron-hole pairs in the top 2–3-μm-thick layer, their consequent diffusion toward a *p-n* junction and separation by junction's built-in field.

This research was supported in part by IMD and NATO (CLG Grant No. 983122).

[1] *Lead Chalcogenides. Physics and Applications*, edited by D. Khokhlov (Taylor & Francis, New York, 2003).
[2] A. Rogalski, Prog. Quantum Electron. **27**, 59 (2003).
[3] A.V. Butenko, V. Sandomirsky, R. Kahatabi, Z. Dashevsky, V. Kasiyan, and Y. Schlesinger, Phys. Rev. Lett. **100**, 057603 (2008).
[4] M. P. Dariel, Z. Dashevsky, A. Jarashneli, S. Shusterman, and A. Horowitz, J. Cryst. Growth **234**, 164 (2002).
[5] Z. Dashevsky, V. Kasiyan, E. Mogilko, A. Butenko, R. Kahatabi, S. Genikhov, V. Sandomirsky, and Y. Schlesinger, Thin Solid Films **516**, 7065 (2008).
[6] B. A. Volkov, L. I. Ryabova, and D. R. Khokhlov, Phys. Usp. **45**, 819 (2002).
[7] A. Butenko, R. Kahatabi, E. Mogilko, R. Strul, V. Sandomirsky, Y. Schlesinger, Z. Dashevsky, V. Kasiyan, and S. Genikhov, J. Appl. Phys. **103**, 024506 (2008).
[8] H. Zogg, in *Lead Chalcogenides. Physics and Applications*, edited by D. Khokhlov (Taylor & Francis, New York, 2003), p. 587.
[9] A. N. Veis, Z. M. Dashevsky, and M. P. Rulenko, Sov. Phys. Semicond. **24**, 76 (1990).
[10] A. Othonos, J. Appl. Phys. **83**, 1789 (1998).